Orientation Relationship of the Intergrowth $Al_{13}Fe_3$ and $Al_{13}Fe_4$ Intermetallics Determined by Single-Crystal X-ray Diffraction

Yibo Liu [1], Changzeng Fan [1,2,*], Zhefeng Xu [1,2], Ruidong Fu [1,2], Bin Wen [1] and Lifeng Zhang [1,3]

[1] State Key Laboratory of Metastable Materials Science and Technology, Yanshan University, Qinhuangdao 066004, China

[2] Hebei Key Lab for Optimizing Metal Product Technology and Performance, Yanshan University, Qinhuangdao 066004, China

[3] School of Mechanical and Materials Engineering, North China University of Technology, Beijing 100144, China

* Correspondence: chzfan@ysu.edu.cn

Supplementary materials include:

Figure S1 Scanning electron microscope (SEM) micrographs of single crystal sample. EDX analysis was performed for various locations as indicated in Table S1.

Table S1 The EDX results conducted at every scanning location.

Figure S2 The precession images: (a) $Al_{13}Fe_3$-1(0*kl*), (b) $Al_{13}Fe_3$-1(*h*0*l*), (c) $Al_{13}Fe_3$-1(*hk*0), (d) $Al_{13}Fe_4$(0*kl*), (e) $Al_{13}Fe_4$(*h*0*l*), (f) $Al_{13}Fe_4$(*hk*0)

Figure S3 The precession images: (a) $Al_{13}Fe_3$-2(0*kl*), (b) $Al_{13}Fe_3$-2(*h*0*l*), (c) $Al_{13}Fe_3$-2(*hk*0), (d) $Al_{13}Fe_4$(0*kl*), (e) $Al_{13}Fe_4$(*h*0*l*), (f) $Al_{13}Fe_4$(*hk*0)

Figure S4 The precession images: (a) $Al_{13}Fe_3$-1(1*kl*), (b) $Al_{13}Fe_3$-1(*h*1*l*), (c) $Al_{13}Fe_3$-1(*hk*1), (d) $Al_{13}Fe_4$(1*kl*), (e) $Al_{13}Fe_4$(*h*1*l*), (f) $Al_{13}Fe_4$(*hk*1)

Figure S5 The precession images: (a) $Al_{13}Fe_3$-1(2*kl*), (b) $Al_{13}Fe_3$-1(*h*2*l*), (c) $Al_{13}Fe_3$-1(*hk*2), (d) $Al_{13}Fe_4$(2*kl*), (e) $Al_{13}Fe_4$(*h*2*l*), (f) $Al_{13}Fe_4$(*hk*2)

Figure S6 The precession images: (a) $Al_{13}Fe_3$-1(3*kl*), (b) $Al_{13}Fe_3$-1(*h*3*l*), (c) $Al_{13}Fe_3$-1(*hk*3), (d) $Al_{13}Fe_4$(3*kl*), (e) $Al_{13}Fe_4$(*h*3*l*), (f) $Al_{13}Fe_4$(*hk*3)

Figure S7 The precession images: (a) $Al_{13}Fe_3$-1(4*kl*), (b) $Al_{13}Fe_3$-1(*h*4*l*), (c) $Al_{13}Fe_3$-1(*hk*4), (d) $Al_{13}Fe_4$(4*kl*), (e) $Al_{13}Fe_4$(*h*4*l*), (f) $Al_{13}Fe_4$(*hk*4)

Figure S8 The precession images: (a) $Al_{13}Fe_3$-1(5*kl*), (b) $Al_{13}Fe_3$-1(*h*5*l*), (c) $Al_{13}Fe_3$-1(*hk*5), (d) $Al_{13}Fe_4$(5*kl*), (e) $Al_{13}Fe_4$(*h*5*l*), (f) $Al_{13}Fe_4$(*hk*5)

Figure S9 The precession images: (a) $Al_{13}Fe_3$-2(1*kl*), (b) $Al_{13}Fe_3$-2(*h*1*l*), (c) $Al_{13}Fe_3$-2(*hk*1), (d) $Al_{13}Fe_4$(1*kl*), (e) $Al_{13}Fe_4$(*h*1*l*), (f) $Al_{13}Fe_4$(*hk*1)

Figure S10 The precession images: (a) $Al_{13}Fe_3$-2(2*kl*), (b) $Al_{13}Fe_3$-2(*h*2*l*), (c) $Al_{13}Fe_3$-2(*hk*2), (d) $Al_{13}Fe_4$(2*kl*), (e) $Al_{13}Fe_4$(*h*2*l*), (f) $Al_{13}Fe_4$(*hk*2)

Figure S11 The precession images: (a) $Al_{13}Fe_3$-2(3*kl*), (b) $Al_{13}Fe_3$-2(*h*3*l*), (c) $Al_{13}Fe_3$-2(*hk*3), (d) $Al_{13}Fe_4$(3*kl*), (e) $Al_{13}Fe_4$(*h*3*l*), (f) $Al_{13}Fe_4$(*hk*3)

Figure S12 The precession images: (a) $Al_{13}Fe_3$-2(4*kl*), (b) $Al_{13}Fe_3$-2(*h*4*l*), (c) $Al_{13}Fe_3$-2(*hk*4), (d) $Al_{13}Fe_4$(4*kl*), (e) $Al_{13}Fe_4$(*h*4*l*), (f) $Al_{13}Fe_4$(*hk*4)

Figure S13 The precession images: (a) $Al_{13}Fe_3$-2(5*kl*), (b) $Al_{13}Fe_3$-2(*h*5*l*), (c) $Al_{13}Fe_3$-2(*hk*5), (d) $Al_{13}Fe_4$(5*kl*), (e) $Al_{13}Fe_4$(*h*5*l*), (f) $Al_{13}Fe_4$(*hk*5)

In order to determine the single crystal morphology and the proportion of elements in the target sample obtained by sintering, Hitachi S-3400 field emission scanning electron microscope (SEM) was used to observe the morphology of single crystal samples, the elements in the samples were analyzed by energy dispersive X-ray spectroscopy (EDX), which was used in electron microscopy, the types and corresponding contents of the elements were analyzed. Concerning the selected fragment of the single crystal sample, EDX analysis was carried out on six spots (see Figure S2) and the corresponding results are listed in Table S1. In Table S1, the chemical compositions of spot 3 is in good agreement with $Al_{13}Fe_4$ phase, while those of spots 1, 2, 4, 5 and 6 are in good agreement with $Al_{13}Fe_3$ phase.

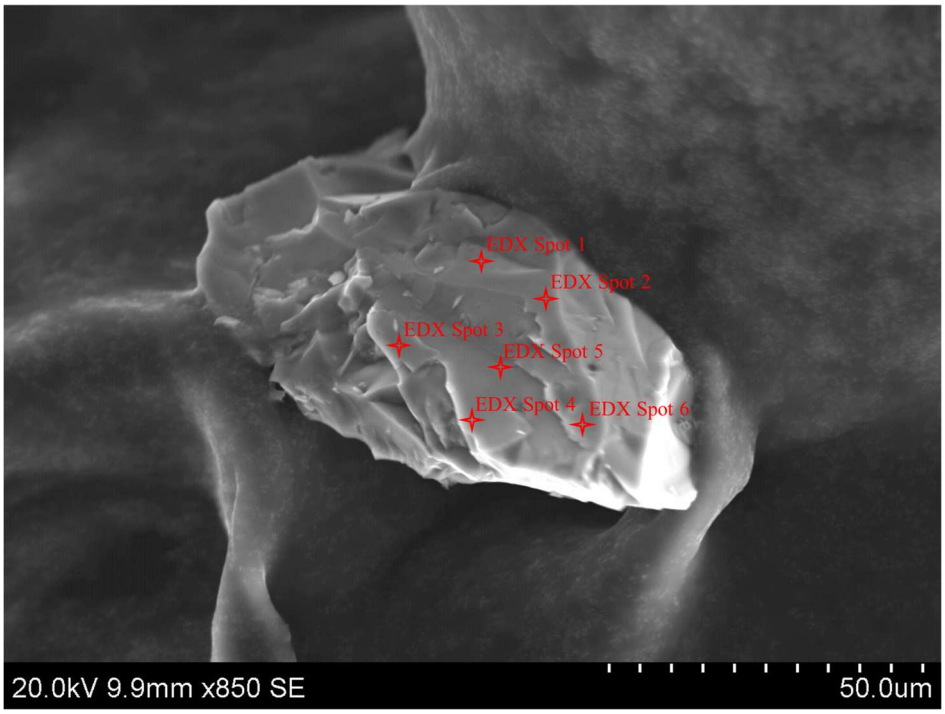

Figure S1 Scanning electron microscope (SEM) micrographs of single crystal sample. EDX analysis was performed for various locations as indicated in Table S1.

Table S1 The EDX results conducted at every scanning location.

	Element	Weight(%)	Atomic(%)	Error(%)	Al:Fe
Spot1	Al	67.33	81.01	4.92	4.27:1
	Fe	32.67	18.99	2.38	
Spot2	Al	67.16	80.99	4.93	4.24:1
	Fe	32.84	19.11	2.37	
Spot3	Al	61.46	76.75	5.34	3.30:1
	Fe	38.54	23.25	2.25	
Spot4	Al	67.64	81.23	4.87	4.33:1
	Fe	32.36	18.77	2.36	
Spot5	Al	67.17	80.90	4.92	4.24:1
	Fe	32.83	19.10	2.36	
Spot6	Al	67.38	81.04	4.89	4.27:1
	Fe	32.63	18.96	2.36	

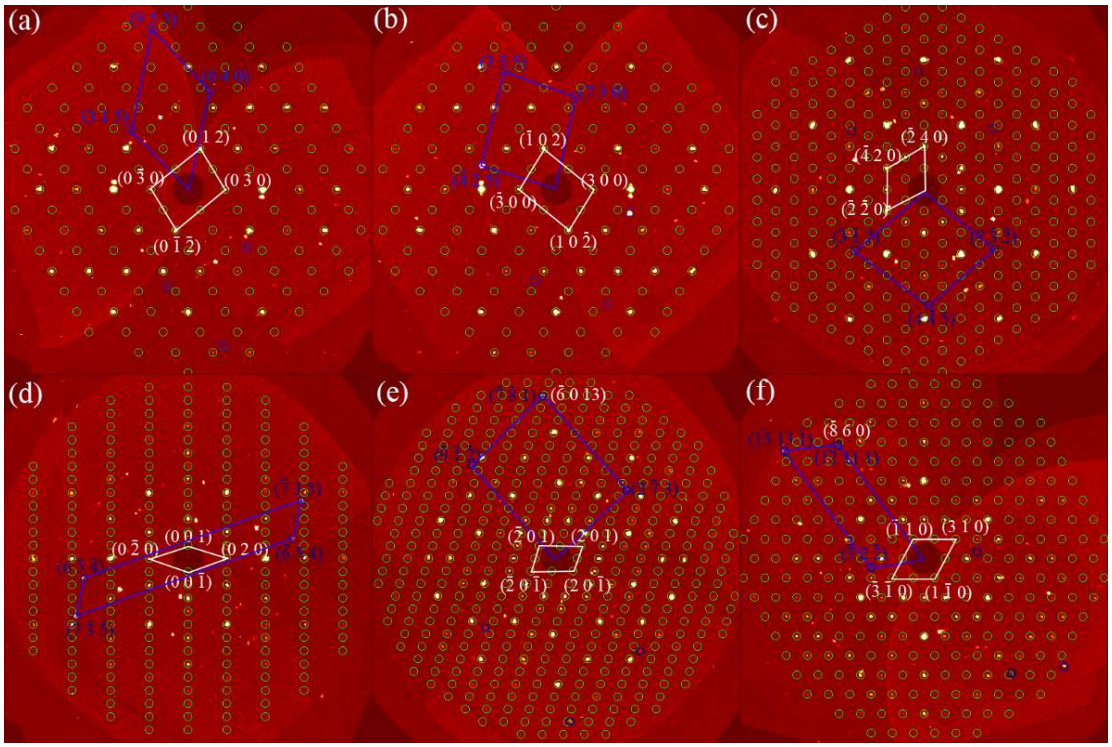

Figure S2 The precession images: (a) $Al_{13}Fe_3$-1(0*kl*), (b) $Al_{13}Fe_3$-1(*h*0*l*), (c) $Al_{13}Fe_3$-1(*hk*0), (d) $Al_{13}Fe_4$(0*kl*), (e) $Al_{13}Fe_4$(*h*0*l*), (f) $Al_{13}Fe_4$(*hk*0).

Figure S2 (a), (b) and (c) represent the precession images of the (0*kl*), (*h*0*l*) and (*hk*0) planes from the $Al_{13}Fe_3$-1 phase while the Figure 10(d), (e) and (f) represent the precession images of the (0*kl*), (*h*0*l*) and (*hk*0) planes from the $Al_{13}Fe_4$ phase. In Figure S2 (a), (b) and (c), the green and blue circle represents the crystal planes of the $Al_{13}Fe_3$-1 phase and the $Al_{13}Fe_4$ phase. While in Figure S2 (d), (e) and (f), the green and blue circle represents the crystal planes of the $Al_{13}Fe_4$ phase and the $Al_{13}Fe_3$-1 phase, respectively. All of the precession images are constructed with a thickness of 0.02 $Å^{-1}$ and a resolution of 0.85 Å. Two kinds of orientation relationships can be found in Figure S2 (e), (f). They are OR1 ($\bar{7}$ $\bar{8}$ 1)$Al_{13}Fe_3$//($\bar{6}$ 0 13)$Al_{13}Fe_4$, [$\bar{17}$ 23 65]$Al_{13}Fe_3$//[0 1 0]$Al_{13}Fe_4$; OR2 ($\bar{12}$ 11 1)$Al_{13}Fe_3$//($\bar{8}$ 6 0)$Al_{13}Fe_4$, [8 9 $\bar{3}$]$Al_{13}Fe_3$//[0 0 1]$Al_{13}Fe_4$.

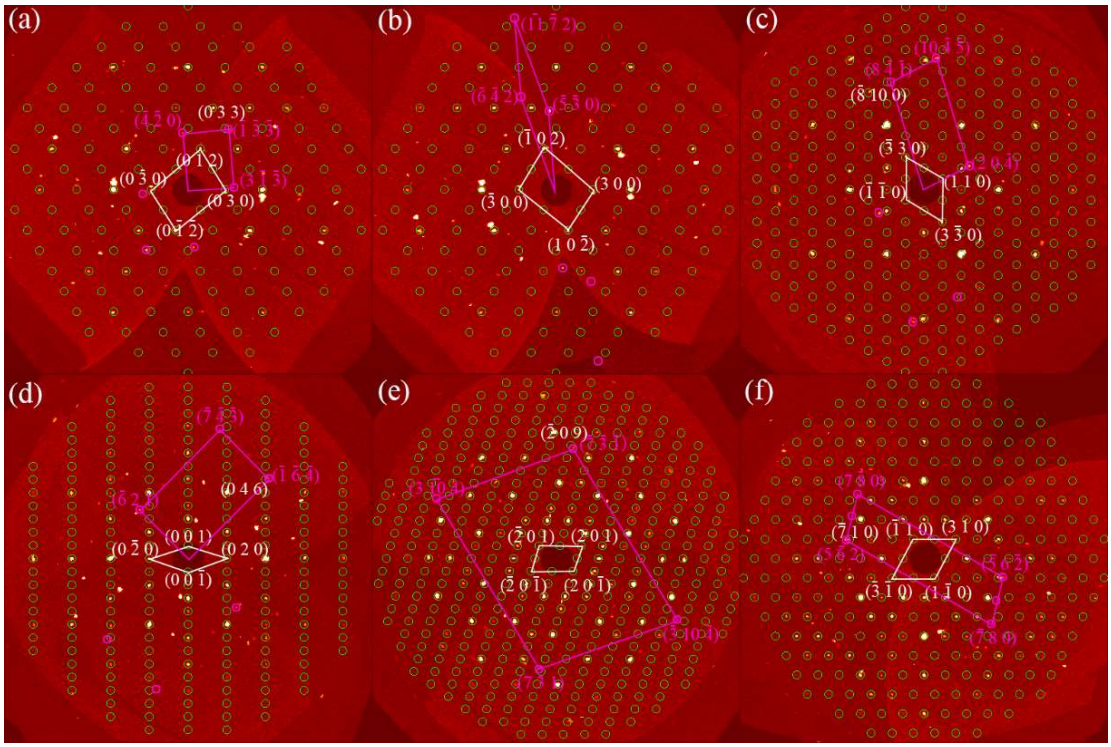

Figure S3 The precession images: (a) $Al_{13}Fe_3$-2(0*kl*), (b) $Al_{13}Fe_3$-2(*h*0*l*), (c) $Al_{13}Fe_3$-2(*hk*0), (d) $Al_{13}Fe_4$(0*kl*), (e) $Al_{13}Fe_4$(*h*0*l*), (f) $Al_{13}Fe_4$(*hk*0)

Figure S3 (a), (b) and (c) represent the precession images of the (0*kl*), (*h*0*l*) and (*hk*0) planes from the $Al_{13}Fe_3$-2 phase while the Figure S3 (d), (e) and (f) represent the precession images of the (0*kl*), (*h*0*l*) and (*hk*0) planes from the $Al_{13}Fe_4$ phase. In Figure S3 (a), (b) and (c), the green and purple circle represents the crystal planes of the $Al_{13}Fe_3$-2 phase and the $Al_{13}Fe_4$ phase, respectively. While in Figure S3 (d), (e) and (f), the green and purple circle represents the crystal planes of the $Al_{13}Fe_4$ phase and the $Al_{13}Fe_3$-2 phase, respectively. All of the precession images are constructed with a thickness of 0.02 $Å^{-1}$ and a resolution of 0.85 Å.

Five kinds of orientation relationships can be found in Figure S3 (a), (c), (d), (e), (f). They are OR3 $(\bar{1}\bar{2}\ 11\ 1)Al_{13}Fe_3//(\bar{8}\ 6\ 0)Al_{13}Fe_4$, $[1\ 0\ 0]Al_{13}Fe_3//[3\ \bar{6}\ 5]Al_{13}Fe_4$; OR4 $(\bar{8}\ 10\ 0)Al_{13}Fe_3//(8\ \bar{4}\ \bar{1})Al_{13}Fe_4$, $[0\ 0\ 1]Al_{13}Fe_3//[8\ 15\ 4]Al_{13}Fe_4$; OR5 $(\bar{1}\ \bar{6}\ \bar{4})Al_{13}Fe_3//(0\ 4\ 6)Al_{13}Fe_4$, $[\bar{2}\ \bar{2}\bar{5}\ 38]Al_{13}Fe_3//[1\ 0\ 0]Al_{13}Fe_4$; OR6 $(\bar{7}\ \ \bar{3}\ \ \bar{1})Al_{13}Fe_3//(\bar{2}\ \ 0\ \ 9)Al_{13}Fe_4$, $[22\ \bar{2}\bar{5}\ \bar{7}\bar{9}]Al_{13}Fe_3//[0\ 1\ 0]Al_{13}Fe_4$; OR7 $(5\ \bar{6}\ 2)Al_{13}Fe_3//(\bar{7}\ 1\ 0)Al_{13}Fe_4$, $[\bar{8}\ \bar{7}\ \bar{1}]Al_{13}Fe_3//[0\ 0\ 1]Al_{13}Fe_4$.

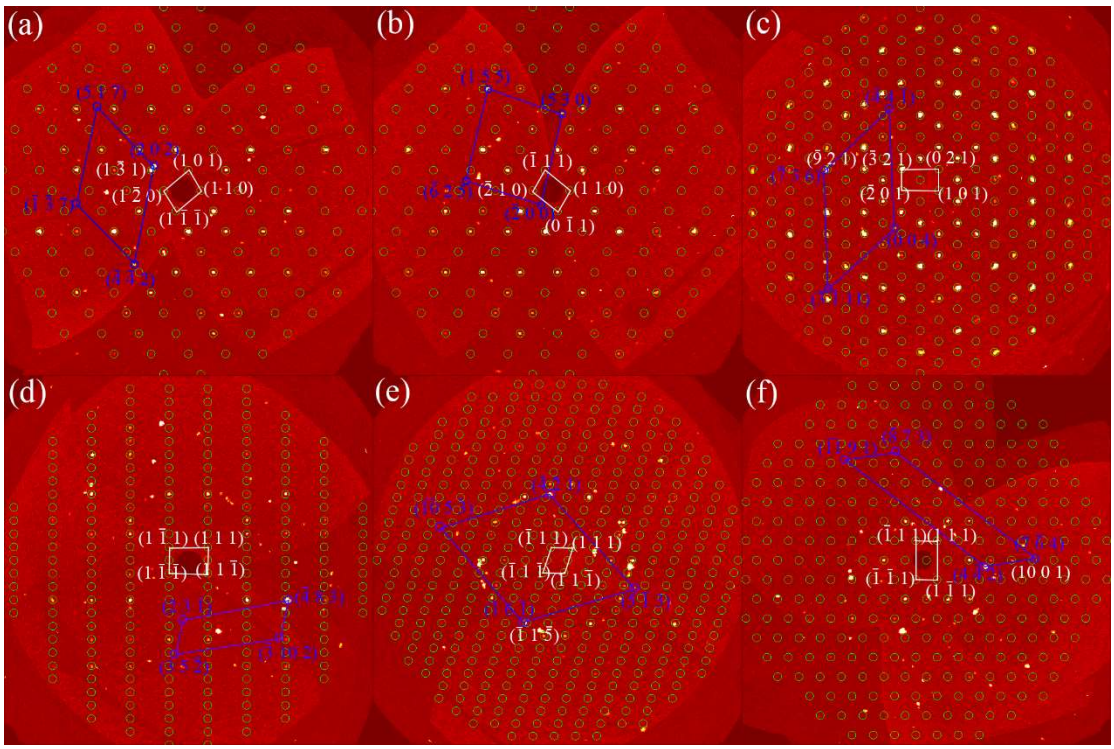

Figure S4 The precession images: (a) $Al_{13}Fe_3$-1(1*kl*), (b) $Al_{13}Fe_3$-1(*h*1*l*), (c) $Al_{13}Fe_3$-1(*hk*1), (d) $Al_{13}Fe_4$(1*kl*), (e) $Al_{13}Fe_4$(*h*1*l*), (f) $Al_{13}Fe_4$(*hk*1).

Figure S4 (a), (b) and (c) represent the precession images of the (1*kl*), (*h*1*l*) and (*hk*1) planes from the $Al_{13}Fe_3$ phase while the Figure S4 (d), (e) and (f) represent the precession images of the (1*kl*), (*h*1*l*) and (*hk*1) planes from the $Al_{13}Fe_4$ phase. In Figure S4 (a), (b) and (c) the green and blue circle represents the crystal planes of the $Al_{13}Fe_3$-1 phase and the $Al_{13}Fe_4$ phase, respectively, the precession images are constructed with a thickness of 0.02 $Å^{-1}$ and a resolution of 0.85 Å. While in Figure S4 (d), (e) and (f) the green and blue circle represents the crystal planes of the $Al_{13}Fe_4$ phase and the $Al_{13}Fe_3$-1 phase, respectively, the precession images are constructed with a thickness of 0.02 $Å^{-1}$ and a resolution of 0.85 Å. Figures S5-S8 use the same Settings as Figure S4. We can find three kinds of crystal plane parallel relationships in Figure S4 (a), (c), (e), (f). They are $(1\bar{3}1)$ $Al_{13}Fe_3$-1//(202) $Al_{13}Fe_4$, $(\bar{9}21)$ $Al_{13}Fe_3$-1//$(\bar{7}36)$ $Al_{13}Fe_4$, $(\bar{1}6\bar{1})$ $Al_{13}Fe_3$-1//$(\bar{1}1\bar{5})$ $Al_{13}Fe_4$, $(7\bar{6}4)$ $Al_{13}Fe_3$-1//(10 0 1) $Al_{13}Fe_4$.

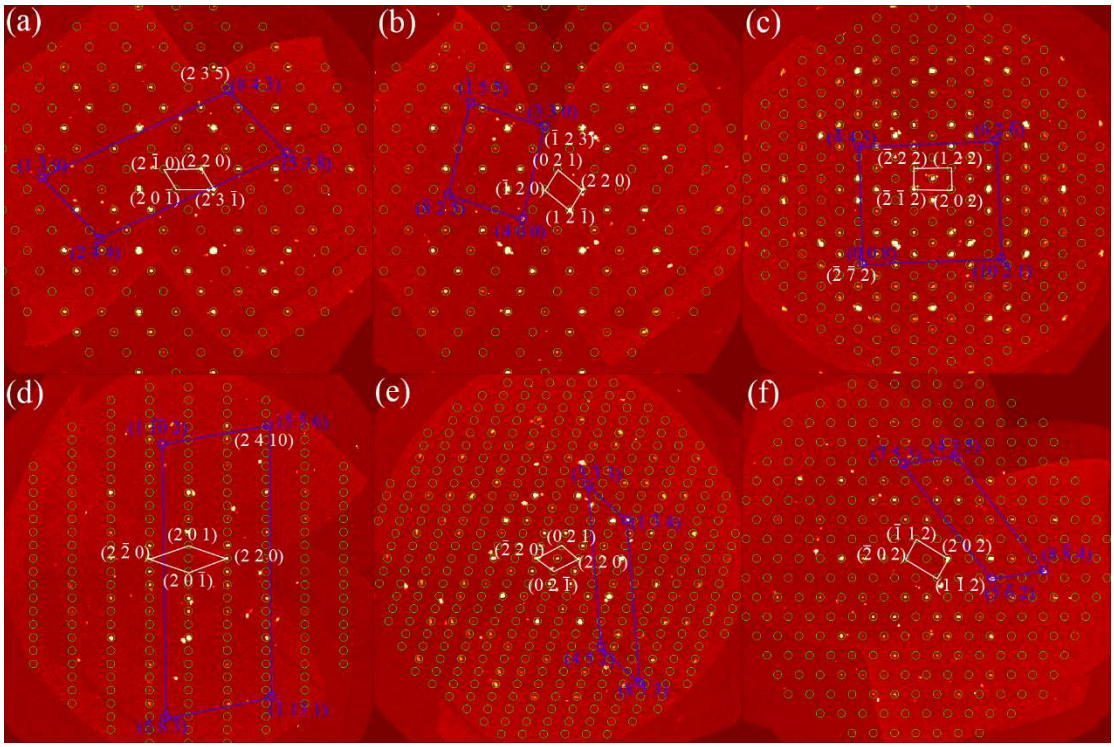

Figure S5 The precession images: (a) $Al_{13}Fe_3$-1(2*kl*), (b) $Al_{13}Fe_3$-1(*h*2*l*), (c) $Al_{13}Fe_3$-1(*hk*2), (d) $Al_{13}Fe_4$(2*kl*), (e) $Al_{13}Fe_4$(*h*2*l*), (f) $Al_{13}Fe_4$(*hk*2).

Figure S5 (a), (b), (c), and (d) show four kinds of crystal plane parallel relationships. They are (235) $Al_{13}Fe_3$-1//(84$\bar{3}$) $Al_{13}Fe_4$, ($\bar{1}$23) $Al_{13}Fe_3$-1//(330) $Al_{13}Fe_4$, ($\bar{2}\bar{7}$2) $Al_{13}Fe_3$-1//(008) $Al_{13}Fe_4$, ($\bar{5}\bar{5}$6) $Al_{13}Fe_3$-1//(2 4 10) $Al_{13}Fe_4$.

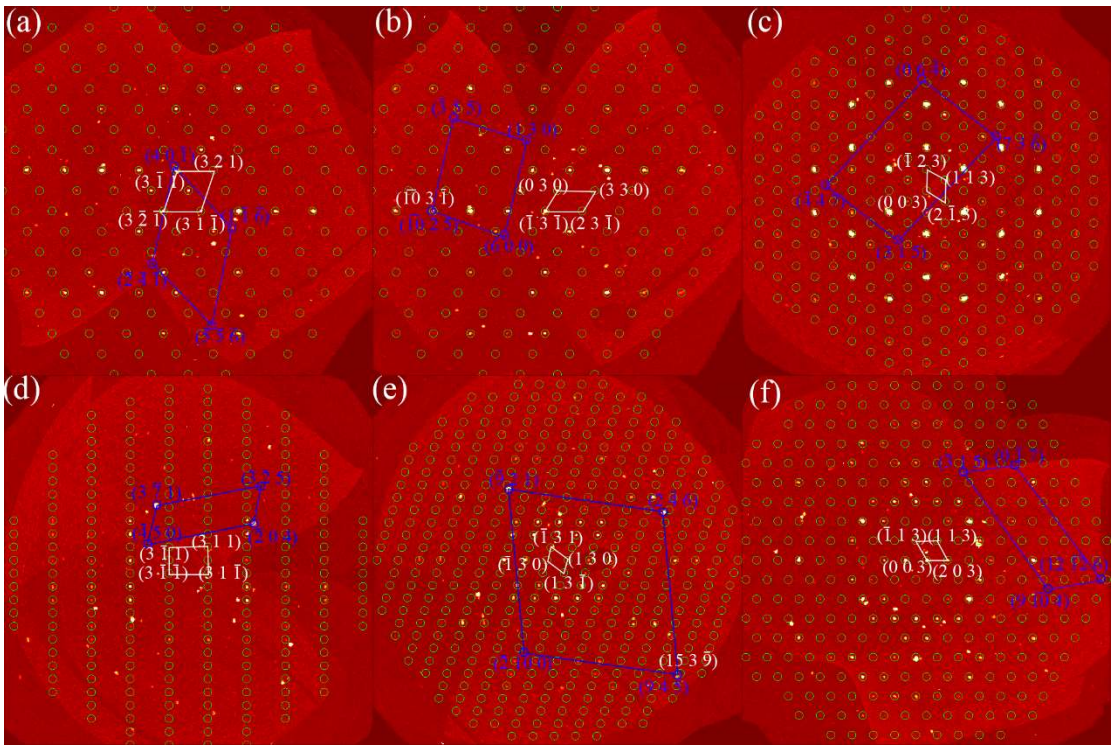

Figure S6 The precession images: (a) $Al_{13}Fe_3$-1(3*kl*), (b) $Al_{13}Fe_3$-1(*h*3*l*), (c) $Al_{13}Fe_3$-1(*hk*3), (d) $Al_{13}Fe_4$(3*kl*), (e) $Al_{13}Fe_4$(*h*3*l*), (f) $Al_{13}Fe_4$(*hk*3).

Figure S6 (a), (b), (e) shows three kinds of crystal plane parallel relationships. They are $(3\bar{1}1)$ $Al_{13}Fe_3$-1//$(40\bar{1})$ $Al_{13}Fe_4$, $(\bar{1}0\bar{3}\bar{1})$ $Al_{13}Fe_3$-1//$(\bar{1}\bar{0}25)$ $Al_{13}Fe_4$, (945) $Al_{13}Fe_3$-1//$(153\bar{9})$ $Al_{13}Fe_4$.

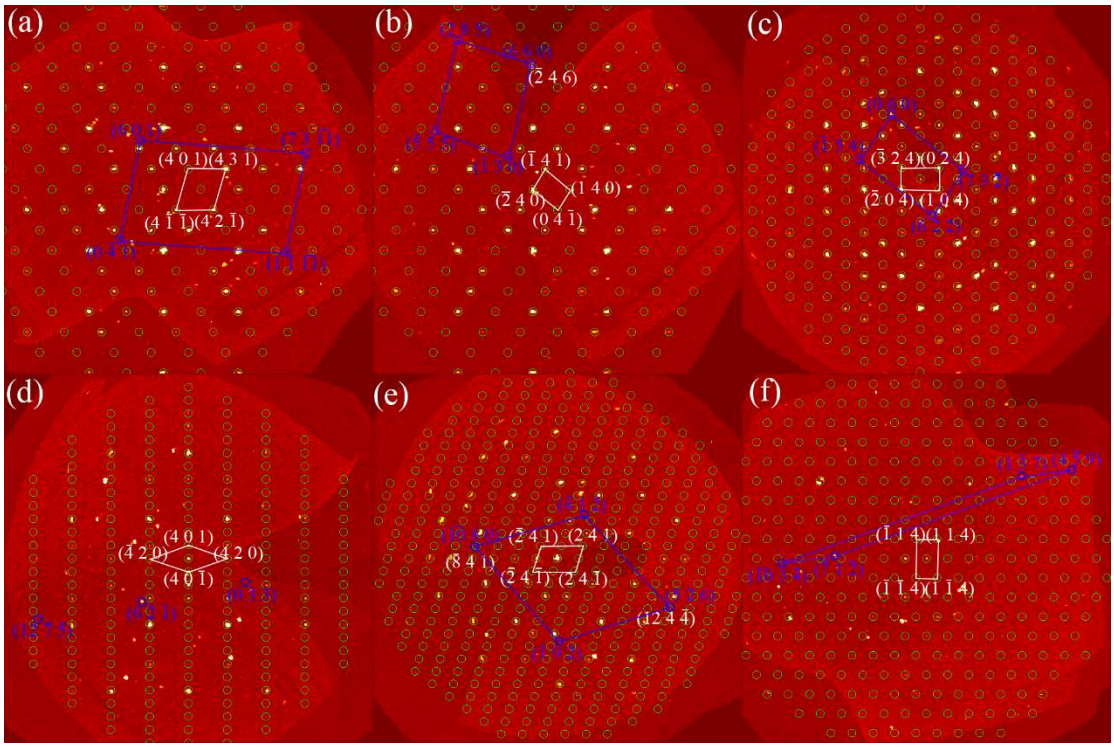

Figure S7 The precession images: (a) $Al_{13}Fe_3$-1(4*kl*), (b) $Al_{13}Fe_3$-1(*h*4*l*), (c) $Al_{13}Fe_3$-1(*hk*4), (d) $Al_{13}Fe_4$(4*kl*), (e) $Al_{13}Fe_4$(*h*4*l*), (f) $Al_{13}Fe_4$(*hk*4).

Figure S7 (b), (e) shows three kinds of crystal plane parallel relationships. They are ($\bar{2}$46) $Al_{13}Fe_3$-1//(660) $Al_{13}Fe_4$, ($\bar{1}$080) $Al_{13}Fe_3$-1//($\bar{8}$41) $Al_{13}Fe_4$, (526) $Al_{13}Fe_3$-1//(12 4 $\bar{4}$) $Al_{13}Fe_4$.

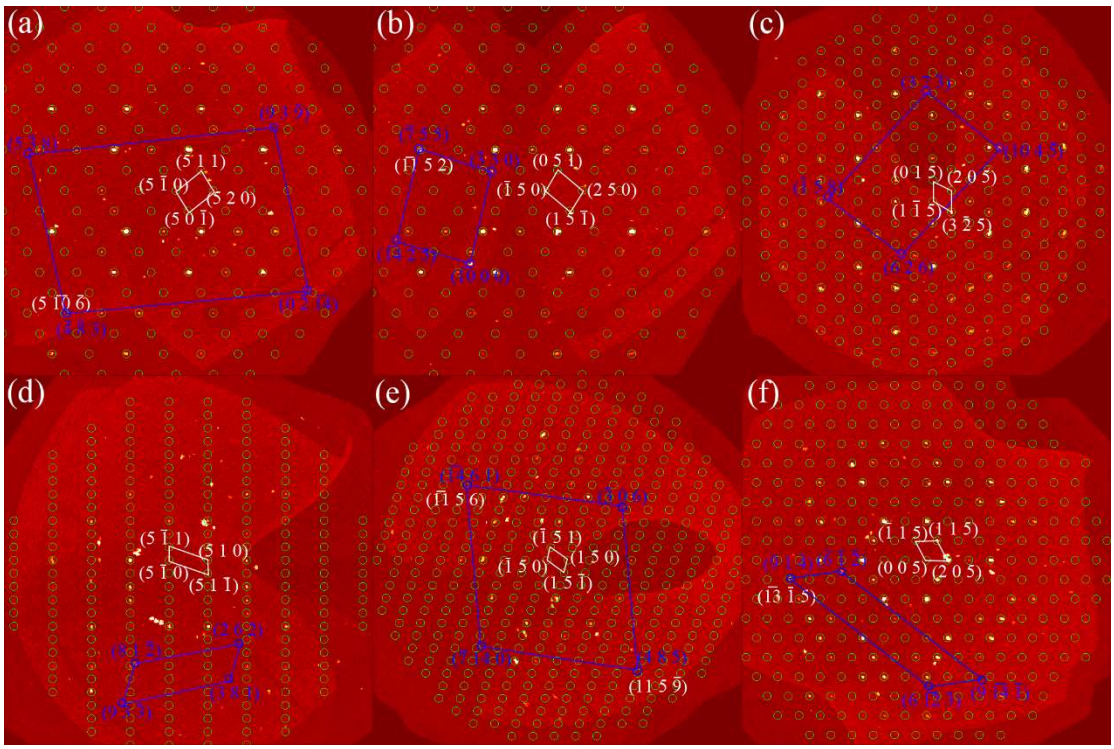

Figure S8 The precession images: (a) $Al_{13}Fe_3$-1(5*kl*), (b) $Al_{13}Fe_3$-1(*h*5*l*), (c) $Al_{13}Fe_3$-1(*hk*5), (d) $Al_{13}Fe_4$(5*kl*), (e) $Al_{13}Fe_4$(*h*5*l*), (f) $Al_{13}Fe_4$(*hk*5).

Figure S8 (a), (b), (e), (f) shows five kinds of crystal plane parallel relationships. It is $(5\bar{1}\bar{0}6)$ $Al_{13}Fe_3$-1//$(\bar{4}\bar{8}3)$ $Al_{13}Fe_4$, $(\bar{1}\bar{1}52)$ $Al_{13}Fe_3$-1//$(\bar{7}55)$ $Al_{13}Fe_4$, $(\bar{1}\bar{4}61)$ $Al_{13}Fe_3$-1//$(\bar{1}\bar{1}56)$ $Al_{13}Fe_4$, (485) $Al_{13}Fe_3$-1//(11 5 $\bar{9}$) $Al_{13}Fe_4$, $(\bar{9}1\bar{4})$ $Al_{13}Fe_3$-1//$(\bar{1}\bar{3}\ \bar{1}5)$ $Al_{13}Fe_4$.

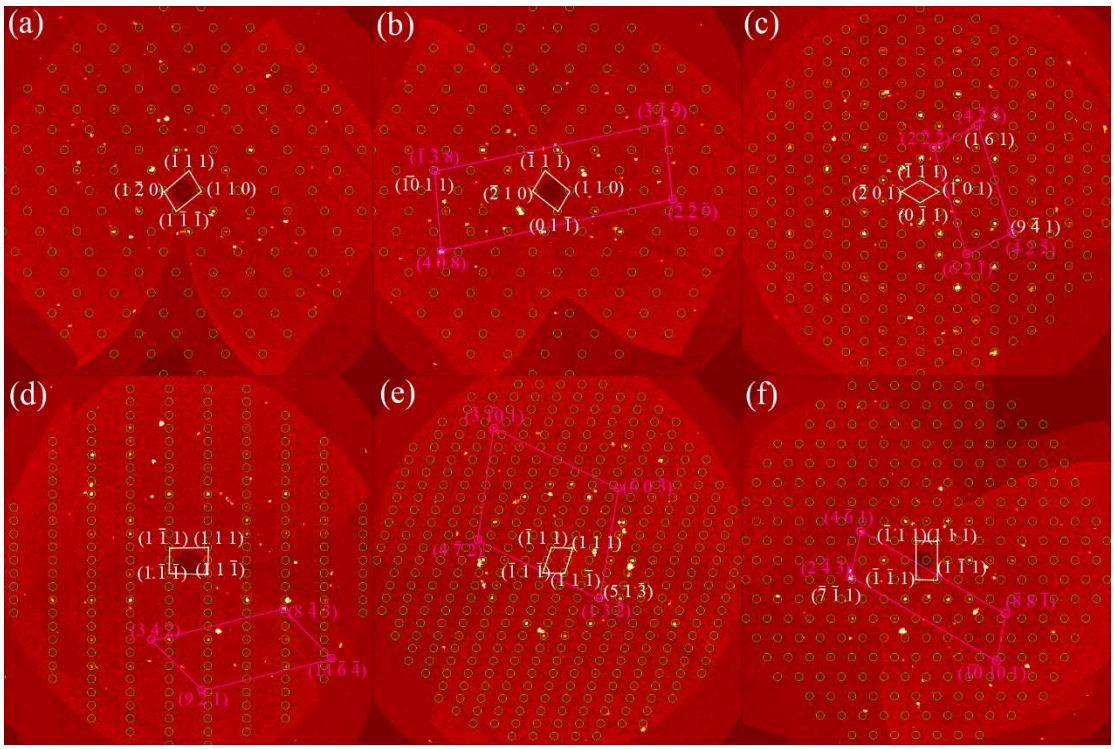

Figure S9 The precession images: (a) $Al_{13}Fe_3$-2(1*kl*), (b) $Al_{13}Fe_3$-2(*h*1*l*), (c) $Al_{13}Fe_3$-2(*hk*1), (d) $Al_{13}Fe_4$(1*kl*), (e) $Al_{13}Fe_4$(*h*1*l*), (f) $Al_{13}Fe_4$(*hk*1).

Figure S9 (a), (b) and (c) represent the precession images of the (1*kl*), (*h*1*l*) and (*hk*1) planes from the $Al_{13}Fe_3$-2 phase while the Figure S9 (d), (e) and (f) represent the precession images of the (1*kl*), (*h*1*l*) and (*hk*1) planes from the $Al_{13}Fe_4$ phase. In Figure S9 (a), (b) and (c) the green and purple circle represents the crystal planes of the $Al_{13}Fe_3$-2 phase and the $Al_{13}Fe_4$ phase, respectively, the precession images are constructed with a thickness of 0.02 $Å^{-1}$ and a resolution of 0.85 Å. While in Figure S9 (d), (e) and (f) the green and purple circle represents the crystal planes of the $Al_{13}Fe_4$ phase and the $Al_{13}Fe_3$-2 phase, respectively, the precession images are constructed with a thickness of 0.02 $Å^{-1}$ and a resolution of 0.85 Å. Figures S10-S13 use the same Settings as Figure S9.

Figure S9 (b), (c), (e), (f) shows five kinds of crystal plane parallel relationships. It is $(\bar{1}\bar{0}11)$ $Al_{13}Fe_3$-2//$(\bar{1}\bar{3}8)$ $Al_{13}Fe_4$, (161) $Al_{13}Fe_3$-2//$(4\bar{2}\bar{6})$ $Al_{13}Fe_4$, $(9\bar{4}1)$ $Al_{13}Fe_3$-2//$(\bar{4}2\bar{5})$ $Al_{13}Fe_4$, $(13\bar{2})$ $Al_{13}Fe_3$-2//$(51\bar{3})$ $Al_{13}Fe_4$, $(2\bar{4}3)$ $Al_{13}Fe_3$-2//$(\bar{7}\,\bar{1}1)$ $Al_{13}Fe_4$.

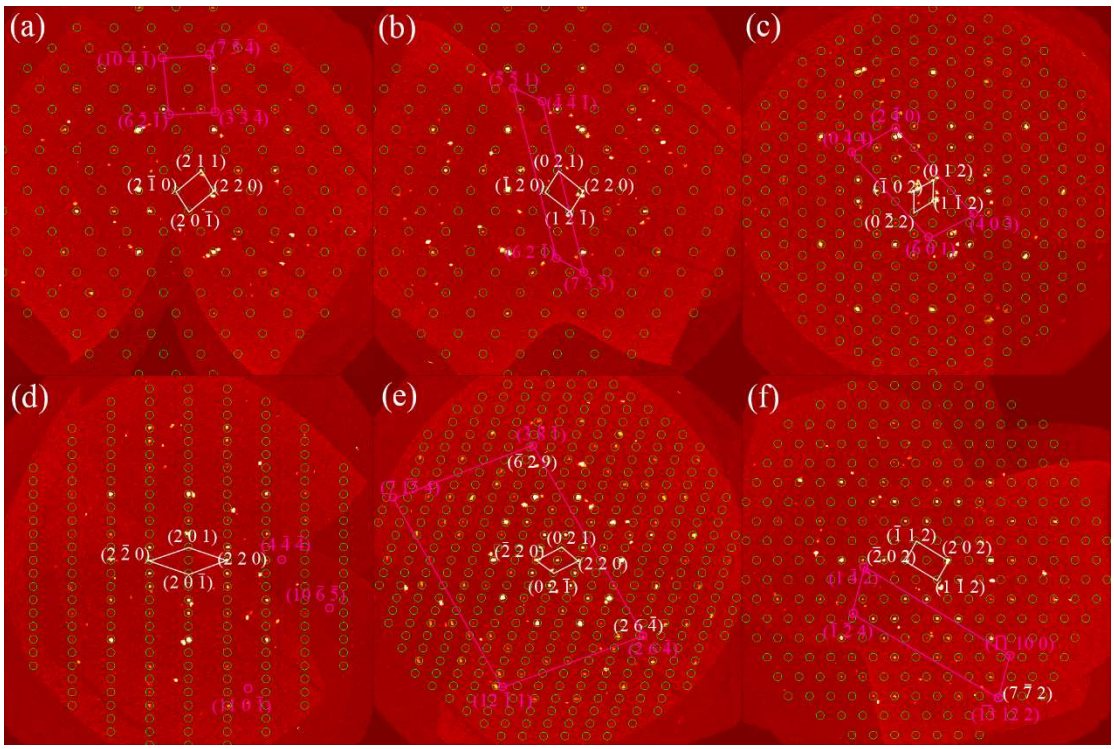

Figure S10 The precession images: (a) $Al_{13}Fe_3$-2(2*kl*), (b) $Al_{13}Fe_3$-2(*h*2*l*), (c) $Al_{13}Fe_3$-2(*hk*2), (d) $Al_{13}Fe_4$(2*kl*), (e) $Al_{13}Fe_4$(*h*2*l*), (f) $Al_{13}Fe_4$(*hk*2).

Figure S10 (e), (f) shows three kinds of crystal plane parallel relationships. It is $(\bar{3}\bar{8}\bar{1})$ $Al_{13}Fe_3$-2//$(\bar{6}29)$ $Al_{13}Fe_4$, $(26\bar{4})$ $Al_{13}Fe_3$-1//(10 2 $\bar{6}$) $Al_{13}Fe_4$, $(\bar{1}\bar{3}\ 12\ 2)$ $Al_{13}Fe_3$-2//$(7\bar{7}2)$ $Al_{13}Fe_4$,

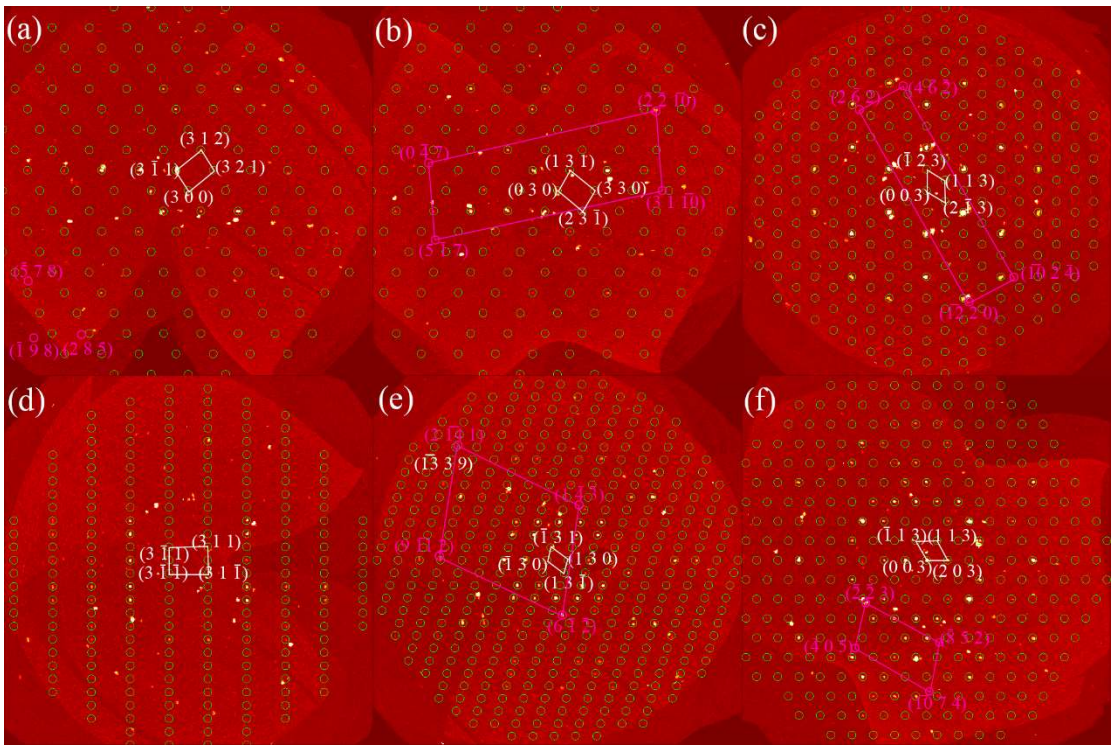

Figure S11 The precession images: (a) $Al_{13}Fe_3$-2(3*kl*), (b) $Al_{13}Fe_3$-2(*h*3*l*), (c) $Al_{13}Fe_3$-2(*hk*3), (d) $Al_{13}Fe_4$(3*kl*), (e) $Al_{13}Fe_4$(*h*3*l*), (f) $Al_{13}Fe_4$(*hk*3).

Figure S11 (e) shows one kinds of crystal plane parallel relationships. It is $(2\bar{1}\bar{4}1)$ $Al_{13}Fe_3$-2//$(\bar{1}\bar{3}39)$ $Al_{13}Fe_4$.

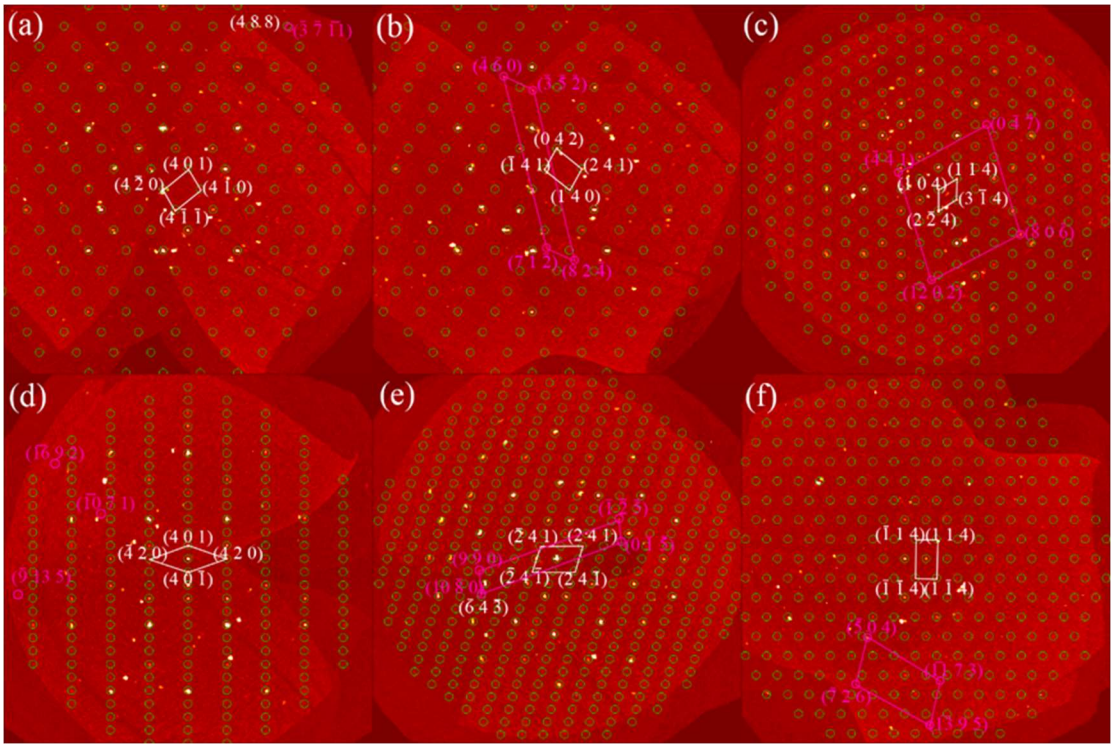

Figure S12 The precession images: (a) $Al_{13}Fe_3$-2($4kl$), (b) $Al_{13}Fe_3$-2($h4l$), (c) $Al_{13}Fe_3$-2($hk4$), (d) $Al_{13}Fe_4$($4kl$), (e) $Al_{13}Fe_4$($h4l$), (f) $Al_{13}Fe_4$($hk4$).

Figure S12 (a), (e) shows two kinds of crystal plane parallel relationships. It is (488) $Al_{13}Fe_3$-2//$(3\bar{7}\bar{1}\bar{1})$ $Al_{13}Fe_4$, $(10\bar{8}0)$ $Al_{13}Fe_3$-2//$(\bar{6}4\bar{3})$ $Al_{13}Fe_4$.

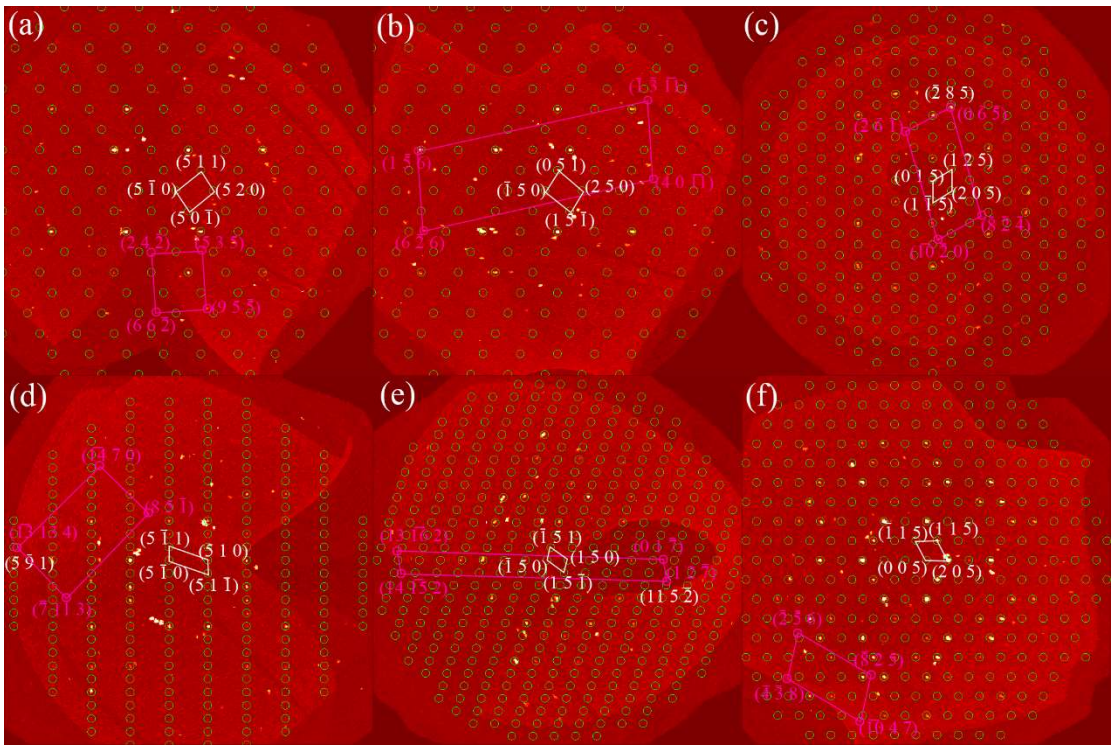

Figure S13 The precession images: (a) $Al_{13}Fe_3$-2(5*kl*), (b) $Al_{13}Fe_3$-2(*h*5*l*), (c) $Al_{13}Fe_3$-2(*hk*5), (d) $Al_{13}Fe_4$(5*kl*), (e) $Al_{13}Fe_4$(*h*5*l*), (f) $Al_{13}Fe_4$(*hk*5).

Figure S13 (c), (d), (e) shows three kinds of crystal plane parallel relationships. It is ($\bar{2}$85) $Al_{13}Fe_3$-2//(0$\bar{6}\bar{5}$) $Al_{13}Fe_4$, ($\bar{1}\bar{3}$13 4) $Al_{13}Fe_3$-2//(5$\bar{9}$1) $Al_{13}Fe_4$, (12$\bar{7}$) $Al_{13}Fe_3$-2//(11 5 $\bar{2}$) $Al_{13}Fe_4$.